

intramolecular and do not depend on  $d$ . Figure 4 shows that  $T_c \sim N(0)$ , in agreement with a recent compilation of lattice constants, calculated densities of states and  $T_c$ 's (21). Given the physical fact we used that most of the coupling is intramolecular, our estimate of  $\lambda$  from the  $H_g$  modes should be as good as the determination of vibration frequencies, that is, good to about 10%. One worry is that our calculation of  $g_m$  is based on the deformations of a  $C_{60}$  molecule, whereas the more appropriate calculation would have a neutralizing background. The Migdal approximation for determining  $T_c$  is only good in our case to  $(\omega_{av}/E_F) \sim 1/5$ .

For low density of states obtainable by small doping, we expect the Coulomb interactions to dominate. In that case the intramolecular Hund's rule coupling (owing to orbital degeneracy) plus the almost empty band usually favors ferromagnetism (28). This may be the simple reason for the recent observation of ferromagnetism in the compound  $TDAE_1C_{60}$  (29).

*Note added in proof:* In recent Raman measurements Duclos *et al.* (30) find that the two highest frequency  $H_g$  phonons, which we find couple most strongly to the electrons (Table 1), are clearly seen in  $C_{60}$  and  $K_6C_{60}$  but disappear in the superconducting compound  $K_3C_{60}$ . This is consistent with our prediction based on Eq. 10 for their linewidth.

#### REFERENCES AND NOTES

1. A. F. Hebard *et al.*, *Nature* **350**, 600 (1991); M. J. Rosseinsky *et al.*, *Phys. Rev. Lett.* **66**, 2830 (1991).
2. R. C. Haddon, L. E. Brus, K. Raghavachari, *Chem. Phys. Lett.* **125**, 459 (1986); M. Ozaki and A. Takahashi, *ibid.* **127**, 242 (1986).
3. S. Satpathi, *ibid.* **130**, 545 (1986).
4. S. Saito and A. Oshiyama, *Phys. Rev. Lett.* **66**, 2637 (1991).
5. J. L. Martins, N. Trouillier, M. Schnabel, preprint (University of Minneapolis, Minnesota, 1991).
6. S. Barisic, J. Labbé, J. Friedel, *Phys. Rev. Lett.* **25**, 419 (1970); C. M. Varma, E. I. Blount, P. Vashista, W. Weber, *Phys. Rev. B* **19**, 6130 (1979); C. M. Varma and W. Weber, *ibid.*, p. 6142.
7. C.-T. Chen *et al.*, *Nature*, in press; J. H. Weaver *et al.*, *Phys. Rev. Lett.* **66**, 1741 (1991); M. B. Jost *et al.*, *Phys. Rev. B*, in press.
8. M. C. O'Brien, *J. Phys. C: Solid State Phys.* **4**, 2524 (1971).
9. In fact, in strong coupling one should consider the true  $n$ -particle states instead of simple product states as assumed in the text. This leads to an increase of phonon phase space, which however affects the 2, 3, and 4 particle states in similar ways. Note that in this case, the low spin states would be considered, and Jahn-Teller interactions thus give rise to a negative Hund's rule coupling.
10. C. M. Varma, *Phys. Rev. Lett.* **61**, 2713 (1988); R. Micnas, J. Ranninger, S. Robaskiewicz, *Rev. Mod. Phys.* **62**, 113 (1990).
11. F. C. Zhang, M. Ogata, T. M. Rice, preprint (University of Cincinnati, Cincinnati, OH, 1991). This paper discusses the possibility that the alkali-ion vibrations may lead to an intramolecular electron-electron attraction. We find this unlikely because they screen their repulsive interactions without screening the attractive interactions. Besides, such vibrations have a frequency

of  $O(200 \text{ cm}^{-1})$ , much smaller than the molecular vibrations we consider and thus are unlikely to be of importance in determining  $T_c$ .

12. G. M. Eliashberg, *Zh. Eksp. Teor. Fiz.* **38**, 966 (1960); *ibid.* **39**, 1437 (1960) *Sov. Phys.-JETP* **11**, 696 (1960); *ibid.* **12**, 1000 (1961).
13. W. L. McMillan, *Phys. Rev.* **167**, 331 (1968).
14. In the derivation of Eq. 9 we missed the factor 5/6 which was kindly pointed out to us by M. Lannoo.
15. M. J. S. Dewar and W. Thiel, *J. Am. Chem. Soc.* **99**, 4899 (1977); *ibid.*, p. 4907.
16. M. D. Newton and R. E. Stanton, *ibid.* **108**, 2469 (1986).
17. R. E. Stanton and M. D. Newton, *J. Phys. Chem.* **92**, 2141 (1988).
18. M. Haesen, J. Almlöf, G. E. Scuseria, *Chem. Phys. Lett.* **181**, 497 (1991); K. Raghavachari and C. M. Rohlfing, *J. Phys. Chem.*, in press.
19. C. S. Yannoni *et al.*, paper presented at the Materials Research Society Meeting, Boston, 1990.
20. D. S. Bethune, *Chem. Phys. Lett.* **179**, 181 (1991).
21. R. M. Fleming, *Nature* **352**, 787 (1991).
22. A. P. Ramirez, M. J. Rosseinsky, D. W. Murphy, R. C. Haddon, in preparation.
23. P. B. Allen and R. C. Dynes, *Phys. Rev. B* **12**, 905 (1975).
24. C. O. Rodriguez *et al.*, *Phys. Rev. B* **42**, 2692 (1990).
25. A. B. Migdal, *Zh. Eksperim. i Teor. Fiz.* **34**, 1438 (1958); *Sov. Phys.-JETP* **7**, 996 (1958).
26. P. Morel and P. W. Anderson, *Phys. Rev.* **125**, 1263 (1962); P. W. Anderson, in preparation.
27. An independent calculation of the electron-phonon

coupling in the Fullerenes has been carried out by M. Schluter *et al.* (in preparation) using a tight-binding method. Our results differ in some ways from theirs. They find the major contribution from the  $\sim 400 \text{ cm}^{-1}$  and  $\sim 1600 \text{ cm}^{-1}$   $H_g$  phonons, where the latter contribution is about half that of the former. In their calculation of  $T_c$  they use an expression averaging over all the phonon frequencies irrespective of their coupling constants.

28. We envisage a competition between Hund's rule couplings and phonon-induced attractive interactions. We note the interesting possibility discussed by S. Chakravarty and S. Kivelson (*Europhys. Lett.*, in press) that in a Hubbard model for  $C_{60}$  clusters, the effective electron-electron interaction is repulsive for small  $U$ ; that is, the Hund's rule is obeyed, but for larger  $U$  it may change sign due to configuration interactions.
29. P. M. Allemand *et al.*, *Science* **253**, 301 (1991).
30. S. J. Duclos, R. C. Haddon, S. Glarum, A. F. Hebard, K. B. Lyons, in preparation.
31. We thank B. Batlogg, R. C. Haddon, S. J. Duclos, I. I. Mazin, M. F. Needels, T. T. M. Palstra, A. P. Ramirez, and M. Schluter for helpful discussions. We particularly thank M. Lannoo for carefully going through the manuscript and pointing out several compensating numerical errors. J.Z. acknowledges financial support by the Foundation of Fundamental Research on Matter (FOM), which is sponsored by the Netherlands Organization for the Advancement of Pure Research (ZWO).

23 August 1991; accepted 3 October 1991

## Long-Term History of Chesapeake Bay Anoxia

SHERRI R. COOPER AND GRACE S. BRUSH

Stratigraphic records from four sediment cores collected along a transect across the Chesapeake Bay near the mouth of the Choptank River were used to reconstruct a 2000-year history of anoxia and eutrophication in the Chesapeake Bay. Variations in pollen, diatoms, concentration of organic carbon, nitrogen, sulfur, acid-soluble iron, and an estimate of the degree of pyritization of iron indicate that sedimentation rates, anoxic conditions and eutrophication have increased in the Chesapeake Bay since the time of European settlement.

SINCE THE OCCURRENCE OF ANOXIA was first reported in the Chesapeake Bay in the 1930's (1), the relative importance of climate versus eutrophication and other anthropogenic influences on the extent and duration of anoxic events has been debated (2-6). Large-scale monitoring of the chemical and physical properties of the Chesapeake Bay began as recently as 1984 (7). Information on the long-term history of anoxia in the Bay is available from stratigraphic records, accessed through paleoecological methods (8). In this report, we describe data from the stratigraphic records to evaluate conditions over time in the mesohaline (moderately brackish) section of the Chesapeake Bay.

Four sediment cores were collected in May 1985 along a transect across the Chesapeake Bay from the Choptank River to Plum Point, Maryland (Fig. 1). This region of the Bay is currently anoxic at least part of

each year. Surface salinities for this area of the Bay average between 8 and 15 parts per thousand (ppt) in spring and fall, respectively; salinities in the bottom water are consistently higher and not usually less than 15 ppt (9). The cores ranged in length from 114 to 160 cm, and have a diameter of 5.7 cm. The sediment in all cores was a relatively uniform mix of gray silt and clay, undisturbed by mixing or bioturbation. Each core was cut into 2-cm intervals. The bottom sediments were dated by the carbon-14 technique and the other samples were dated on the basis of pollen horizons and pollen concentration techniques (10). The agricultural pollen horizon was recognized by a sharp increase in concentration of ragweed pollen in relation to oak pollen and was dated as A.D. 1760 on the basis of historical records of land use in the area. Several controls were used to check the accuracy of both dating methods. For example, a sediment sample taken from above the agricultural pollen horizon in a nearby core could not be dated by radiocarbon

Department of Geography and Environmental Engineering, Johns Hopkins University, Baltimore, MD 21218.

**Table 1.** Averages and standard deviations of sedimentation rates and chemistry data for Chesapeake Transect cores (includes only samples analyzed for chemical parameters); N, number of samples, Sed, sedimentation.

Core	N	Sed rate (cm yr <sup>-2</sup> )	Carbon (% dry wt)	TOC (mg cm <sup>-2</sup> yr <sup>-1</sup> )	N (% dry wt)	N (mg cm <sup>-2</sup> yr <sup>-1</sup> )	S (% dry wt)	S (mg cm <sup>-2</sup> yr <sup>-1</sup> )	DOP	HCl-Fe (mg g)	HCl-Fe (mg cm <sup>-2</sup> yr <sup>-1</sup> )
R4-30	4	0.12 ± 0.04	1.67 ± 0.26	0.81 ± 0.39	0.15 ± 0.03	0.07 ± 0.04	0.57 ± 0.08	0.27 ± 0.07	0.20 ± 0.04	20.9 ± 6.2	0.96 ± 0.24
R4-45	11	0.03 ± 0.01	1.68 ± 0.05	0.25 ± 0.06	0.19 ± 0.01	0.03 ± 0.01	1.17 ± 0.14	0.18 ± 0.05	0.33 ± 0.04	21.6 ± 4.9	0.33 ± 0.12
R4-50	13	0.05 ± 0.01	1.74 ± 0.05	0.39 ± 0.12	0.17 ± 0.02	0.04 ± 0.01	1.25 ± 0.12	0.29 ± 0.11	0.31 ± 0.03	20.7 ± 2.4	0.48 ± 0.19
50-E	4	0.04 ± 0.02	1.49 ± 0.18	0.34 ± 0.18	0.14 ± 0.00	0.03 ± 0.02	0.67 ± 0.31	0.16 ± 0.10	0.25 ± 0.11	16.9 ± 1.9	0.40 ± 0.21
R4-30	6	0.31 ± 0.16	2.63 ± 0.84	2.58 ± 0.86	0.23 ± 0.07	0.23 ± 0.09	0.81 ± 0.21	0.86 ± 0.39	0.21 ± 0.04	26.7 ± 2.4	2.75 ± 0.92
R4-45	11	0.22 ± 0.03	2.10 ± 0.93	1.62 ± 0.93	0.20 ± 0.03	0.17 ± 0.06	1.24 ± 0.26	1.05 ± 0.35	0.34 ± 0.01	21.9 ± 5.8	1.81 ± 0.52
R4-50	20	0.29 ± 0.11	2.59 ± 0.44	2.90 ± 1.12	0.25 ± 0.04	0.28 ± 0.01	1.71 ± 0.15	1.94 ± 0.67	0.39 ± 0.05	22.6 ± 5.2	2.63 ± 1.21
50-E	4	0.17 ± 0.07	1.74 ± 0.06	1.35 ± 0.63	0.16 ± 0.01	0.12 ± 0.05	0.60 ± 0.19	0.48 ± 0.28	0.21 ± 0.05	19.5 ± 1.5	1.57 ± 0.81

methods; this example indicates that there were no errors caused by the presence of old-carbon or reservoir effects (11). The more important post-European dates determined by pollen methods in the Bay have been compared to <sup>210</sup>Pb methods for 13 cores in the Potomac estuary and were shown to be in reasonable agreement. Where there were discrepancies, independent evidence corroborated the pollen-derived date (12).

Oxidation and other chemical processes in sediments are affected by oxygen availability in the bottom waters, sedimentation rates, and availability of organic C (13). The paleoecological indicators used to assess changes in available oxygen over time and changes in the eutrophic state of the ecosystem (characterized by high-nutrient loading) include diatoms, total and organic C (TOC), total and organic N, total S, acid-soluble Fe, and an estimate of the degree of pyritization of Fe (DOP). Diatoms are particularly useful for paleoecological research because they grow a morphologically species-specific silica shell, which is preserved in the sediments.

Measured TOC is the amount of organic detritus preserved in the sediment. Preservation of organic matter reflects the balance between initial input with deposition and loss due to bacterially mediated decomposition. Input of C to the sediment is a function of both the concentration of organic matter and the rate of sediment deposition. In the mesohaline section of the Chesapeake Bay, phytoplankton biomass accumulation contributes to TOC, which fuels oxygen depletion in the spring and contributes to the maintenance of hypoxic and anoxic conditions during the summer months (6). Nutrient input to the estuary has been directly correlated with spring phytoplankton biomass, and benthic oxygen demand has been correlated with death and sedimentation of the phytoplankton (6). Increased sedimentation rates change oxidant availability and increase the length of time C has to react at any given depth interval (13). Eutrophic conditions would be expected to increase the concentrations of highly reactive organic matter in the form of phytoplankton biomass (6, 13). The rate of bacterial decomposition of C in the sediment is a function of the geochemical nature of the organic matter (that is, its reactivity), the nature of the oxidant available (for example, oxygen, nitrate, sulfate, and so forth), and the availability or rate of transport of the oxidant to the sediment. Anaerobic C oxidation in the sediments of the mesohaline portion of the Chesapeake Bay is accomplished in part by abundant sulfate-

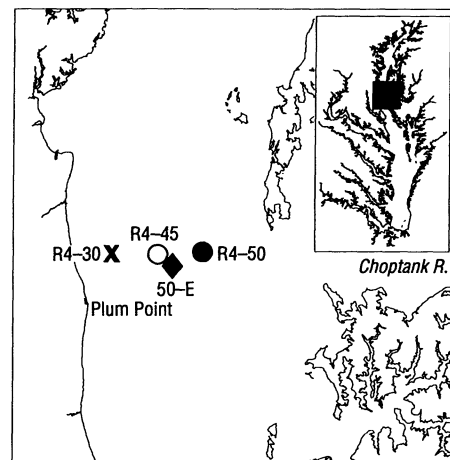


**Fig. 1.** Location of sediment cores collected in the mesohaline midsection of the Chesapeake Bay. Core R4-30 was collected under 10 m of water on the western shelf of the Bay. Cores R4-45, R4-50, and 50-E were collected under 14, 16, and 16 m of water, respectively, on either side of the main channel of the Bay.

reducing bacteria. Sulfides produced by these bacteria may escape to the water column as highly toxic H<sub>2</sub>S or be incorporated in the sediments through combination with metals such as Fe to produce Fe monosulfides and eventually pyrite (14). At higher sedimentation rates, parts of the S cycle are more insulated from the water column, and sulfide mineral species are more likely to be preserved in the sediments. Under eutrophic conditions, concentrations and reactivity of TOC are increased, oxidants are consumed at a higher rate, and the geochemical environment changes. This change is expressed in the nature of the authigenic mineral suite, most significantly the sulfide minerals.

Raiswell *et al.* (15) have used the parameter DOP to determine the degree of bottom-water oxygenation at the time of deposition in organic-bearing sediments. DOP is the ratio of pyritic Fe to total reactive Fe. Raiswell *et al.* found that aerobic samples (DOP < 0.42) could be clearly separated from restricted samples (water with low oxygen concentrations; 0.46 < DOP < 0.80), but that restricted and inhospitable (water with little or no oxygen present; 0.55 < DOP < 0.93) categories overlapped. Their results show that oxygen availability in ancient paleoenvironments is more effectively discriminated by DOP than by TOC and C-S relations. Middleburg (16) presented and reviewed measurements of DOP in recent sediments, showing that these data are consistent with the DOP model of Raiswell *et al.* (15).

Both dried and ashed (17) sediment samples were measured for percent C, N, and S on a CNS analyzer (18). Acid-soluble Fe

was measured with the use of atomic absorption spectrophotometry on samples boiled in HCl for 1 min (15). The S content was assessed for only the nonashed samples because ashing reduces the actual values of the inorganic S content. Earlier measurements of concentration and speciation of S in 696 samples of Chesapeake Bay sediments in Maryland showed that S is in the form of inorganic reduced S (19).

As a result of sample handling and storage of these cores, exact S speciation could not be determined. Consequently, total S was used to estimate pyritic S (hence pyritic Fe) in the sediments to obtain DOP, because pyrite is the ultimate authigenic reservoir for sedimentary S (14, 15, 20, 21).

The sediment chemistry data show that the composition of the sediments and sedimentation conditions have changed in the

Chesapeake Bay since the time of European settlement (Table 1; Figs. 2 to 4). On the basis of pollen techniques (10) and radiocarbon dating, sedimentation rates increased fivefold to sevenfold since European settlement in cores R4-45, R4-50, and 50-E and 1.5 times in core R4-30. Average rates before settlement ranged from 0.03 to 0.14 cm yr<sup>-1</sup>, compared with 0.13 to 0.27 cm yr<sup>-1</sup> after settlement. These calculated rates correspond well with other measurements of recent and Holocene sedimentation rates for the Chesapeake Bay (22, 23). Increased sedimentation brings with it input from terrestrial sources, including nutrients, clay, and silt, which have a high affinity for organic matter.

The TOC was 95 to 100% of the total C measured for all of the sediment samples except one, which may have contained shell material. Measured TOC levels were between 1.3 and 4.1% of total dry sediment weight. Concentrations of TOC were converted to yearly preservation of TOC in the sediments with the use of the appropriate sedimentation rates. The highest level, 4.96 mg cm<sup>-2</sup> yr<sup>-1</sup>, occurred at 8-cm depth and was dated at A.D. 1948 in core R4-50 (Fig. 5). Total nitrogen (TN) was 84 to 100% organic N and was linearly related to TOC. The highest TN levels were 0.32% of the dry weight, and the highest level of N preservation was 0.54 mg cm<sup>-2</sup> yr<sup>-1</sup>, after 1940. Changes in TOC and N as a function of time cannot be readily modeled with the use of accepted decay models for reduction in marine sediments (13) because of large variations in TOC preservation since European settlement. The higher preservation of TOC since European occupation suggests that sedimentation rates or eutrophication have increased. These conclusions are supported by the pollen, diatom, S, and DOP results.

Sulfur levels of <1.0% dry weight and estimated DOP values of <0.42 in cores R4-30 and 50-E indicate that sedimentation conditions have been aerobic during most of each year both before and after European settlement. Because core R4-30 was farthest from the main channel and under shallower water than the other cores, this result was expected. Core 50-E differs from cores R4-45 and R4-50 possibly because it was collected in a different methane gas zone (24) and it contained slightly coarser grained sediment than the other nearby cores. The presence of gas in the sediments affects the bulk chemistry and in particular the TOC and S chemistry (24). In cores R4-45 and R4-50 the S concentration was >1.0% dry weight and in core R4-50, the S concentration increased from 1.25 ± 0.12% before 1760 to 1.71 ± 0.15% since European settlement (Table

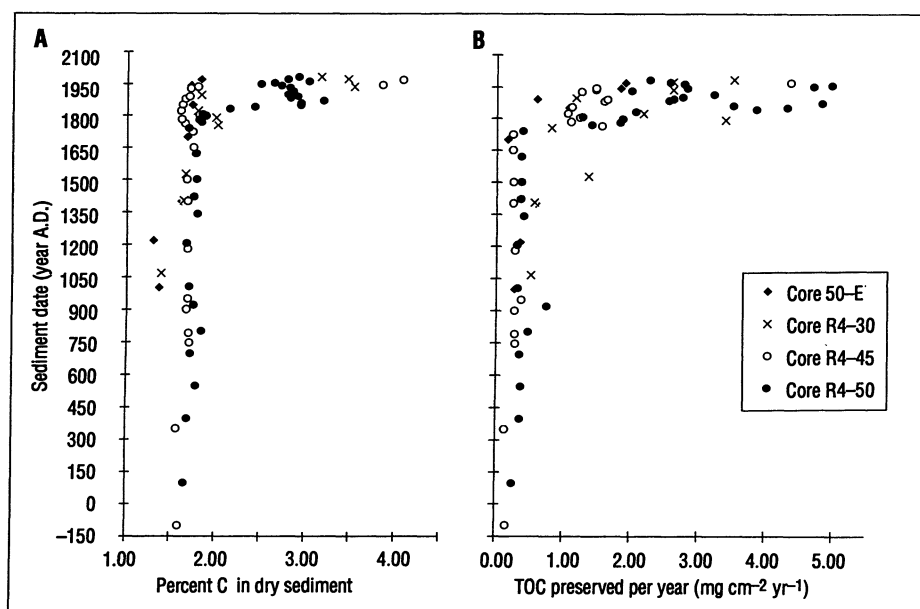


**Fig. 2.** (A) Percent C per gram dry sediment for each sample as measured on the CNS analyzer for the four cores collected. (B) Corrected preservation of organic C in the sediments. These values were calculated by multiplying the raw data by the appropriate sedimentation rates determined for each sample (10). The data are graphed by the date assigned to each sediment sample according to pollen and radiocarbon methods.

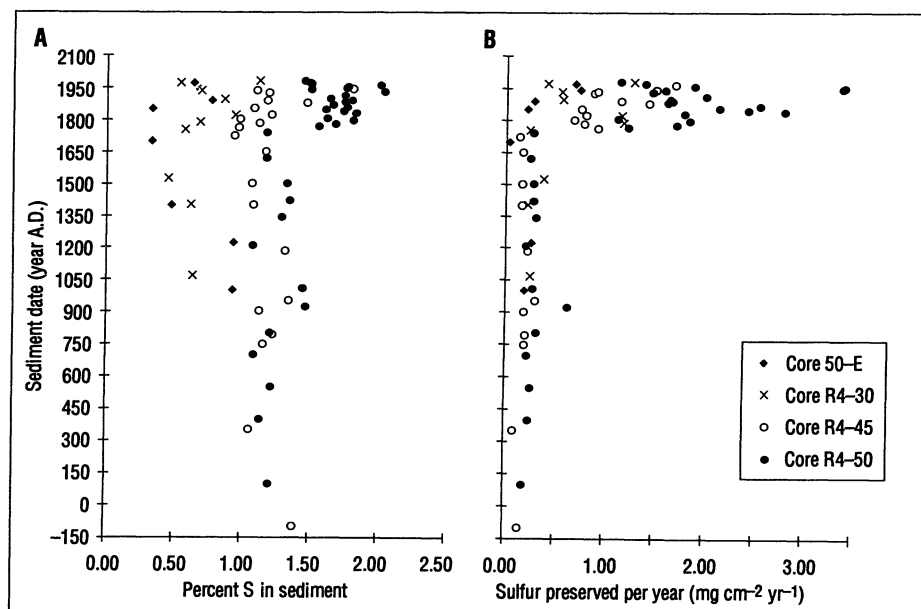


**Fig. 3.** (A) Percent S per gram dry sediment for each sample as measured on the CNS analyzer for the four cores collected. (B) Corrected preservation of S in the sediments. These values were calculated by multiplying the raw data by the appropriate sedimentation rates determined for each sample (10).

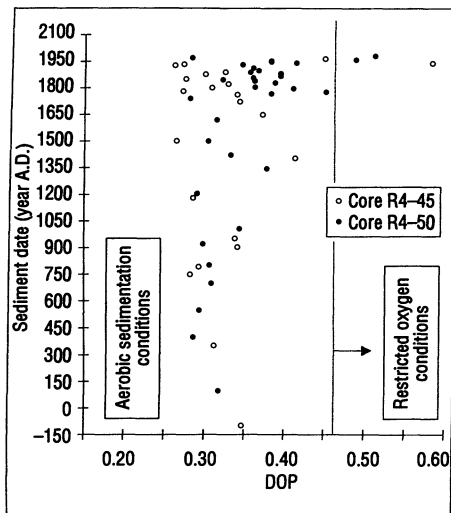


**Fig. 4.** Estimates of the parameter DOP (degree of pyritization of iron) as calculated for each of the samples in the two cores collected that showed DOP > 0.46 in any of the more recent sediments. In the Chesapeake Bay, restricted oxygen conditions are not maintained year round. Therefore, a DOP > 0.46 may indicate that anoxic conditions prevailed for part of each year represented by that sediment sample. Three post-1940 samples show estimated DOP values > 0.46.

1). After adjustment of these values for sedimentation rates, S preservation is seen to have increased from an average of  $0.29 \pm 0.11 \text{ mg cm}^{-2} \text{ yr}^{-1}$  before 1760 to a high of  $3.41 \text{ mg cm}^{-2} \text{ yr}^{-1}$  after 1940 (Fig. 6). In addition, three measurements of estimated DOP values of > 0.46 in these cores indicate that there has been a relative

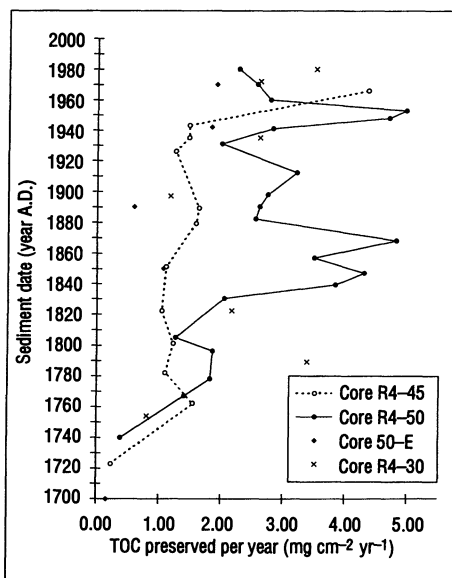


**Fig. 5.** Preservation of carbon in the sediments dated 1700 to 1980. Points are connected for cores R4-45 and R4-50 because they were sampled in more detail for this time period than cores 50-E and R4-30.

change in bottom-water conditions since 1940 (Fig. 4). The dates assigned to the sediments with high DOP values were centered around 1943 in core R4-45 and around 1960 and 1980 in core R4-50. With continued availability of reactive Fe and organic C for sulfate-reducing bacteria to use, DOP values of the more recent sediments should increase even more with time.

The diatom data show that the total number of species and overall community diversity as measured by Shannon's  $H'$  (25) have decreased and the relative abundance of centric to pennate species (which are generally planktonic or free-floating and benthic or bottom-dwelling species, respectively), have increased since European settlement. For example, in cores R4-50 and R4-45, diversity before European settlement, consistently measured as  $H' = 3.8$ , began to show some decrease in the late 1700's and reached its lowest point in the most recent sediments at  $H' = 2.3$  in R4-50 and  $H' = 2.5$  in R4-45. In core R4-45, there were 100 species identified before 1760 and 68 species in the most recent sediments, and there has been a large increase in the percentage of the planktonic *Cyclotella* species (from 20 to 65% of the diatoms counted). The centric to pennate diatom ratio (used as an index of eutrophication) for this core changed from 1.3 before European settlement to 5.2 in the most recent sediments. These trends indicate that the ecosystem has been more stressed since European settlement and subjected to an increased nutrient input.

Initial European settlement in the region of the Chesapeake Bay extended from the early 17th to early 18th century. After initial land clearance, deforestation was rapid, culminating with over 80% of the land cleared in the period from 1830 to 1880, accompanied by deep plowing during the period of intensive agriculture. At the same time, there was a greater freshwater flow to the Bay because of increased river discharge (26). This land use resulted in a doubling of sediment accumulation in the estuarine tributaries. Since the mid-19th century, sediment transported into the estuary carried with it nutrients from heavy applications of fertilizers. In addition to non-point source sediment and nutrients, sewage discharge and, more recently, industrial waste discharge into many of the tributaries and the Bay contribute to high local nutrient and pollutant input.

The data from the cores show that sedimentation rates and sediment chemistry have changed in the Chesapeake Bay since the time of initial land clearance for agri-

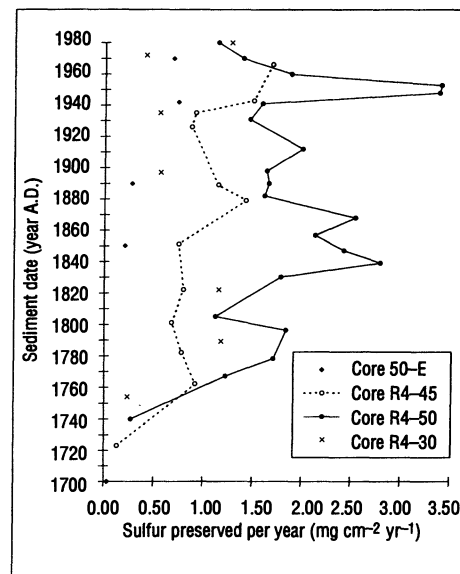


**Fig. 6.** Preservation of S in the sediments dated 1700 to 1980. Points are connected for cores R4-45 and R4-50 because they were sampled in more detail for this time period than cores 50-E and R4-30.

culture. DOP values, S chemistry, and diatom assemblages show that the ecology of the Bay has also changed since 1940. These alterations may be due to industrialization and urbanization, or the cumulative effect of increasing eutrophication and increased river discharge since deforestation began. These conditions set the stage for greater oxygen depletion in the Bay and more production of toxic  $\text{H}_2\text{S}$  in years of high spring precipitation when stratification of the water column is more intense (3).

#### REFERENCES AND NOTES

1. C. L. Newcombe and W. A. Horn, *Science* **88**, 80 (1938).
2. C. B. Officer *et al.*, *ibid.* **223**, 22 (1984).
3. H. H. Seliger, J. A. Boggs, W. H. Biggley, *ibid.* **228**, 70 (1985).
4. J. L. Taft, E. O. Hartwig, R. Loftus, *Estuaries* **3**, 242 (1980).
5. H. H. Seliger and J. A. Boggs, in *Understanding the Estuary: Advances in Chesapeake Bay Research. Proceedings of a Conference*, M. P. Lynch, E. C. Krome, Eds. (Chesapeake Research Consortium, Solomons, MD, 1988), pp. 111-127.
6. T. C. Malone, in *Oxygen Dynamics in Chesapeake Bay: A Synthesis of Recent Research*, D. Smith, M. Leffler, G. Mackiernan, Eds. (Maryland Sea Grant, College Park, MD, in press).
7. R. Batuik, in *Dissolved Oxygen in the Chesapeake Bay: Processes and Effects*, G. B. Mackiernan, Ed. (Maryland Sea Grant, College Park, MD, 1987), pp. 12-17.
8. G. S. Brush, *J. Wash. Acad. Sci.* **76**, 146 (1986).
9. D. W. Pritchard, *J. Mar. Res.* **2**, 106 (1952).
10. G. S. Brush, *Limnol. Oceanogr.* **34**, 1235 (1989). Carbon-14 dating was done by Beta Analytic Inc., Miami, FL. The agricultural pollen horizon (AH) was identified in each core and dated as A.D. 1760. In core R4-45, the sample from 106 to 114 cm was carbon-14 dated as  $2260 \pm 100$  years before present (ybp), and AH is at 50 cm. In core R4-50, the sample from 156 to 160 cm was dated as 2160 ybp.

and AH is at 60 cm. In core 50-E, the bottom sample from 126 to 128 cm was dated as  $2650 \pm 160$  ybp and AH is at 30 cm. In core R4-30, the sample from 148 to 150 cm was dated as  $910 \pm 130$  ybp and AH is at 50 cm. Average sedimentation rates between the bottom carbon-14 dated sediment, the agricultural horizon, and the surface sediment (dated A.D. 1985, the time of core collection) were adjusted according to the pollen concentration in each 2-cm interval to give the sedimentation rate for each interval. In the method, we assumed that pollen influx was uniform during periods of similar vegetation cover and species composition for both the pre-European period and the post-European period. Because pollen grains are Stokesian particles, hydrodynamically similar to fine sediment, their transport in water is also similar to fine sediment. The majority of the pollen enters the estuary from the atmosphere. Rates of sediment accumulation then correspond inversely to pollen concentration, and can be calculated for each interval (in this case 2 cm) of the core, with the equation  $R_{0-2} = \bar{n}/n_{0-2}\bar{R}$ , where  $R_{0-2}$  is the sedimentation rate for 0-2 cm,  $\bar{n}$  is the average number of pollen grains per dated interval,  $\bar{R}$  is the average sedimentation rate ( $d/t$ ) for the dated interval,  $d$  is the depth of a dated horizon in the core, and  $t$  is the time in years of the dated horizon. Once the sedimentation rates are calculated for each interval of a core, a chronology was established by dividing the depth of the interval by the sedimentation rate for that interval, giving the number of years represented.

11. G. M. MacDonald, R. P. Beukens, W. E. Kieser, *Ecology* **72**, 1150 (1991).
12. G. S. Brush, E. A. Martin, R. S. DeFries, C. A. Rice, *Quat. Res.* **18**, 196 (1982).
13. R. A. Berner, *Colloq. Int. C.N.R.S.* **293**, 35 (1980).
14. M. B. Goldhaber and I. R. Kaplan, in *The Sea*, Vol. 5, E. D. Goldberg, Ed. (Wiley, New York, 1962), pp. 569-655.
15. R. Raiswell, F. Buckley, R. A. Berner, T. F. Anderson, *J. Sediment. Petrol.* **58**, 812 (1988).
16. J. J. Middleburg, *Geochim. Cosmochim. Acta* **55**, 815 (1991).
17. M. D. Krom and R. A. Berner, *J. Sediment. Petrol.* **53**, 660 (1983).
18. A Carlo-Erba CNS Analyzer at the Maryland Geological Survey, Baltimore, Maryland, was used to analyze all samples. Replicates of every seventh sample were always within 0.1% and usually within 0.01%. Calibration standards used were estuarine sediment samples of known TOC, N, and S content provided by the Maryland Geological Survey. Organic C and organic N were calculated as the difference between dried and ashed sediment sample measurements of C and N.
19. E. L. Hennessee, P. J. Blakeslee, J. M. Hill, *J. Sediment. Petrol.* **56**, 674 (1986).
20. R. A. Berner, *Geochim. Cosmochim. Acta* **48**, 605 (1984).
21. C. J. Lord and T. M. Church, *ibid.* **47**, 1381 (1983).
22. J. F. Donoghue, *Quat. Res.* **34**, 33 (1990).
23. C. B. Officer, D. R. Lynch, G. H. Setlock, G. R. Helz, in *The Estuary as a Filter*, V. S. Kennedy, Ed. (Academic Press, New York, 1984), pp. 131-157.
24. J. M. Hill, J. P. Halka, R. D. Conkwright, K. Kocot, J. Park, *Continental Shelf Res.*, in press.
25. H. G. Washington, *Water Res.* **18**, 653 (1984). The Shannon-Wiener index ( $H'$ ) is the most widely used diversity index in ecology.  $H' = \sum(n_i/n) \ln(n_i/n)$ , for  $i = 1$  to  $s$ , where  $H'$  is the community diversity,  $n$  is the total number of organisms per sample,  $n_i$  is the number of individuals per taxon and  $s$  is the total number of species in a unit area (or volume).
26. J. M. Bosch and J. D. Hewlett, *J. Hydrol.* **55**, 3 (1982).
27. Support for this research was furnished by Maryland Sea Grant grant R/P-22 (NOAA). We acknowledge the participation of R. Biggs, K. Eisner, T. Yerkes, and C. Ward, and thank J. Park, D. Wells, and L. Hennessee. We thank J. Hill for help in preparation of the manuscript, and A. Stone, T. Malone, J. Cornwall, G. Helz, and H. Seliger, for reviews.

31 May 1991; accepted 21 August 1991

## Magma Generation on Mars: Amounts, Rates, and Comparisons with Earth, Moon, and Venus

RONALD GREELEY AND BYRON D. SCHNEID

Total extrusive and intrusive magma generated on Mars over the last ~3.8 billion years is estimated at  $654 \times 10^6$  cubic kilometers, or 0.17 cubic kilometers per year ( $\text{km}^3/\text{yr}$ ), substantially less than rates for Earth (26 to  $34 \text{ km}^3/\text{yr}$ ) and Venus (less than  $20 \text{ km}^3/\text{yr}$ ) but much more than for the Moon ( $0.025 \text{ km}^3/\text{yr}$ ). When scaled to Earth's mass the martian rate is much smaller than that for Earth or Venus and slightly smaller than for the Moon.

EXPLORATION OF MARS IN THE LAST two decades has shown that volcanism was important in the evolution of this terrestrial planet (1-4). Images of its surface reveal a variety of volcanic landforms, including vast lava plains and shield volcanoes more than 500 km across. Strong  $\text{Fe}^{2+}$  absorptions in spectral reflectance measurements of the surface indicate that much of the surface has a mafic composition (5). Soil x-ray fluorescence spectra suggest that parent rocks were also probably basaltic (6). Photogeologic mapping (7-9) shows that volcanic units cover at least half of Mars' surface and that volcanism was important from the terminal stages of heavy bombardment and initial crustal formation through the formation of the geologically younger surfaces seen today.

Because volcanism appears to be dominant in the evolution of Mars, an assessment of the history of magma generation and comparison of that history with other terrestrial planets is warranted. Although deriving a complete history must await more data, such as in situ measurements of the full range of compositions on Mars, significant progress can be made with information currently available. Earlier studies (10, 11) made initial estimates of the volcanic materials erupted on Mars through time. Those studies were limited, however, in that the thicknesses of lava flows making up the martian plains were assumed to average 1 km; moreover, there was no attempt to determine the amounts of magma generated as intrusive materials but not erupted. We address both of these limitations in this report.

To determine the amounts of magma produced through time on Mars, we (i) mapped exposed volcanic materials to determine their areal extent; (ii) estimated their thicknesses using the techniques of De Hon (12) for lava plains and published topography for volcanic constructs and the Tharsis region; (iii) assigned ages to the mapped units (7-9) using impact crater distributions; (iv) determined volumes from (i) and

(ii); (v) extrapolated volcanic volumes by age for areas covered by younger rocks, on the basis of the work of Tanaka *et al.* (11); and (vi) inferred the amounts of intrusive magmas on the basis of ratios of intrusive to-extrusive materials on Earth (13). We then derived the rate of magma production on Mars and compared the results with rates estimated for Venus, Earth, and the Moon.

We used photographic mosaics of Mars (14) as bases for mapping exposed volcanic materials. Units and ages previously defined on small-scale maps (7-9) were reassessed and modified as appropriate. We took a conservative approach in that we excluded some smooth, featureless plains previously interpreted as volcanic deposits where we could not identify distinctive volcanic features. Consequently, we estimate that the total area of Mars surfaced with volcanic units is  $66.2 \times 10^6 \text{ km}^2$ , or 46% of the surface, somewhat less than earlier estimates. Two methods were used to determine the volumes of exposed volcanic materials. For large volcanic constructs and the Tharsis Rise (the major volcanic province), volumes were derived directly from the topography (14). Topographic data were combined with paleostratigraphic reconstructions taken partly from Scott and Tanaka (15) in order to partition the volumes as a function of geologic age. Most (82.4% by area) exposed

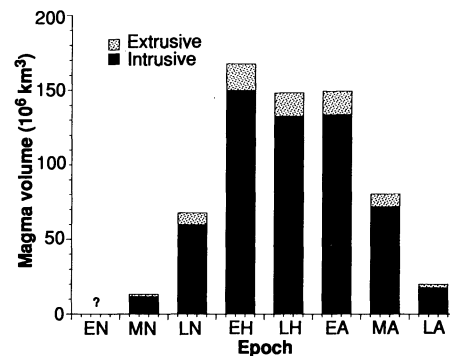


Fig. 1. Histogram of intrusive, extrusive, and total magma production for each martian epoch; EN, Early Noachian; MN, Middle Noachian; LN, Late Noachian; EH, Early Hesperian; LH, Late Hesperian; EA, Early Amazonian; MA, Middle Amazonian; LA, Late Amazonian.

Department of Geology, Arizona State University, Tempe, AZ 85287.